Acta Acustica united with Acustica
Vol. 102 (2016) 1108 – 1117

DOI 10.3813/AAA.919022

A New EEMD-Based Scheme for Detection of Insect Damaged Wheat Kernels Using Impact Acoustics

Min Guo[1)], Yuting Ma[1)], Zichen Zhao[2)], Miao Ma[1)], Xiaojun Wu[1)], Richard W. Mankin[2)]
[1)] School of Computer Science, Shaanxi Normal University, Xi'an 710062, China. guomin@snnu.edu.cn
[2)] US Department of Agriculture, Agricultural Research Service, Center for Medical, Agricultural, and Veterinary Entomology, Gainesville, FL 32608, USA

Summary
Internally feeding insects inside wheat kernels cause significant, but unseen economic damage to stored grain. In this paper, a new scheme based on ensemble empirical mode decomposition (EEMD) using impact acoustics is proposed for detection of insect-damaged wheat kernels, based on its capability to process non-stationary signals and its suppression of mode mixing. The intrinsic mode function (IMF) kurtosis, IMF form factors, IMF third-order Rényi entropies, and the mean of the degree of stationarity were extracted as discriminant features used as the inputs to a support vector machine (SVM) for non-linear classification. In these experiments, 98.7% of undamaged wheat kernels and 93.3% of insect-damaged ones were correctly detected, which indicated the effectiveness of the proposed method for categorizing undamaged wheat kernels from insect-damaged wheat kernels (IDK).

PACS no. 43.60.-c

1. Introduction

Stored grain suffers severe damage due to hidden, internally feeding insects [1]. In addition, insects cause nutritional losses and contamination by excrement and fragments. Therefore, the work of detection of insect-damaged wheat kernels (IDK) is of great urgency. Previously, a variety of methods have been explored to detect the insects inside the wheat kernels, such as x-ray imaging, acoustic detection of larval movement and chewing, and carbon dioxide monitoring [2]. However, most of these methods are either slow, labor intensive, expensive, or cannot quantitatively measure insect infestation levels [2]. To find more efficient and convenient methods, detection techniques based on impact acoustics have been studied by many researchers.

Originally, detection techniques based on impact acoustics were applied to separate pistachio nuts with closed shells from those with open shells [3]. After the work by Pearson et al, improved procedures for sorting pistachios were studied [4, 5, 6, 7, 8]. In addition, detection techniques based on impact acoustics were used to separate fully developed from underdeveloped hazelnuts [9], separate undamaged from damaged/cracked hazelnut kernels [10], remove shell pieces from hazelnut kernels [11], discriminate between potato tubers and clods [12, 13], and separate filled and empty walnuts [14].

The detection system used for sorting pistachio nuts, [3], was improved to detect IDK [2]. The features of the signals, both in the time domain and frequency domain, were extracted by three approaches. First, a time-domain signal model was developed with Weibull curve fitting. The method achieved 88.8% detection accuracy for undamaged wheat kernels and 86.6% for insect-damaged ones. Second, the time-domain variances in short-time windows were computed, enabling 85.2% of undamaged wheat kernels and 76.2% of insect-damaged ones to be classified correctly. Third, the frequency spectra magnitudes were obtained through discrete Fourier transform (DFT). It was reported that the detection accuracies of undamaged wheat kernels and IDK were 87.4% and 85.0% respectively. When the three methods were combined to extract features, and linear discriminant analysis (LDA) was used for classification, the classification accuracies of undamaged wheat kernels and IDK were 98.0% and 84.4% respectively [2].

Pearson, Cetin, Tewfik and Haff developed a non-destructive, real-time device to detect insect damage, sprout damage, and scab damage in wheat kernels [15]. They emphasized that the maximum amplitudes of the acoustic emission signals from wheat kernels could not play a decisive role in distinguishing each type of signal. However, compared with the signals from undamaged wheat kernels, the signals from IDK had a longer reso-

Received 2 November 2014,
accepted 20 September 2016.

nance duration. For further study, in addition to the discriminant features used before, the differential spectrum and the maxima in short-time windows were used as discriminant features, and the stepwise discriminant analysis routine was exploited for selecting a small feature subset. Using a neural network, 98% of undamaged wheat kernels and 87% of insect-damaged ones were correctly classified. In addition to high accuracy, the new sorting method provided celerity, with a throughput of 40 wheat kernels/s.

On this basis, a new adaptive time-frequency analysis and classification method using impact acoustics was proposed to separate three types of damaged wheat kernels (IDK, pupal, and scab) from undamaged wheat kernels [16]. Discriminant features were extracted from the adaptively segmented acoustic signal and were post-processed by principal component analysis (PCA). Using a linear discriminant classifier, these three types of damaged wheat kernels were separated from undamaged ones with 96%, 82%, and 94% accuracies respectively. Furthermore, the algorithm presented adaptation capability to the time-frequency patterns of signals, making it a more universal method for grain kernel classification.

In this report, a new scheme based on EEMD using impact acoustics is proposed for detection of IDK. The discriminant features, including the IMF kurtosis, IMF form factors, IMF third-order Rényi entropies, and the mean of the degree of stationarity are extracted as the inputs into a SVM classifier and the resultant detection accuracy is measured.

2. Experimental apparatus

Figure 1 shows the experimental apparatus for dropping wheat kernels onto an impact plate and collecting the impact acoustic signals. The experimental apparatus includes a vibration feeder, an impact plate, a microphone, and a computer equipped with a sound card. The impact sounds are affected by the structural properties of the substrate. To compare suitabilities of different substrates, 2000 wheat kernels were tested, 700 on glass, 700 on wood, and 600 on stainless steel plates. The differences between fluctuation properties of the signals from undamaged wheat kernels and IDK during the resonance decay process were larger when using stainless steel, so the impact plate was determined to be a block of stainless steel. The dimensions were adjusted to maximize the resonance properties of the impact plates, which ultimately were set at approximately 24 × 11 × 0.06 cm. Then, 600 wheat kernels, including 300 undamaged wheat kernels and 300 IDK, were used in the experiment. To avoid the circumstance that the wheat kernels bounce twice before leaving the impact plate, the incline angle was set 30° above the horizontal and the drop distance from the feeder to the impact plate was set at 50 cm through trial and error.

The impact acoustic signals were collected by using a condenser microphone (SHURE BG 4.1). The microphone was connected to a computer equipped with a sound card (MAYA44), sampling at 48 kHz with 18-bit resolution.

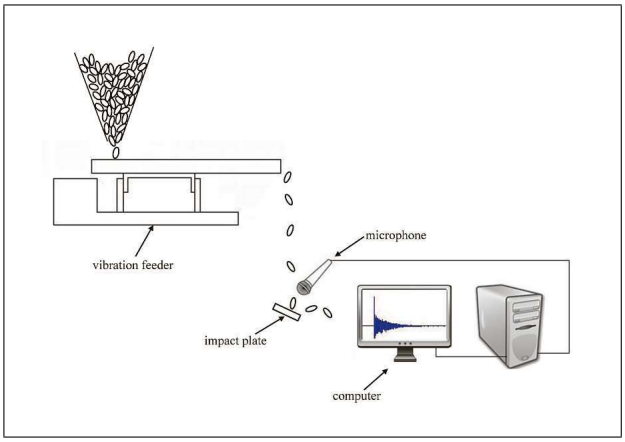

Figure 1. Schematic of experimental apparatus.

By using the vibration feeder, the wheat kernels were channeled into a single-file stream. The freely falling wheat kernels impacted the stainless steel, and the impact acoustic signals were acquired and saved in the computer.

3. Signal processing

Traditional time-frequency analysis methods, such as the short-time Fourier transform (STFT), Wigner-Ville distribution (WVD), as well as the wavelet transform (WT), are not very suitable for processing non-stationary and non-linear signals because of lack of self-adaptive basis functions. Huang, Shen, and Long et al put forward a method, the Hilbert-Huang transform, whose core is empirical mode decomposition (EMD), which is able to process the non-stationary and non-linear signals [17]. However, the problem of mode mixing cannot be avoided, which is the primary drawback of EMD.

To overcome the problem of mode mixing in EMD, a new method called ensemble empirical mode decomposition (EEMD) was proposed [18]. EEMD is based on the local characteristic time scales of a signal, and the signal can be self-adaptively decomposed into several IMFs, where each of the IMF components contains a different local characteristic time scale. Unlike EMD, the finite white noise, which is uniformly full of the whole time-frequency plane, is added to the signal by using EEMD. Then the components of signals in different scales are automatically separated into appropriate scales of reference. With sufficient numbers of trials, the white noise can be eliminated to achieve better decomposition results [18]. Based on its capability for suppressing mode mixing, EEMD is widely used in the field of fault diagnosis [19, 20], and signal detection [21].

The EEMD algorithm can be described as follows:

1. Add a white noise series to the original signal to obtain a general signal,

$$X_i(t) = x(t) + \omega_i(t), \qquad i = 1, 2, \ldots, K, \qquad (1)$$

where $x(t)$ represents the original signal, $\omega_i(t)$ is the ith added white noise series, and $X_i(t)$ is the general signal of the ith trial.

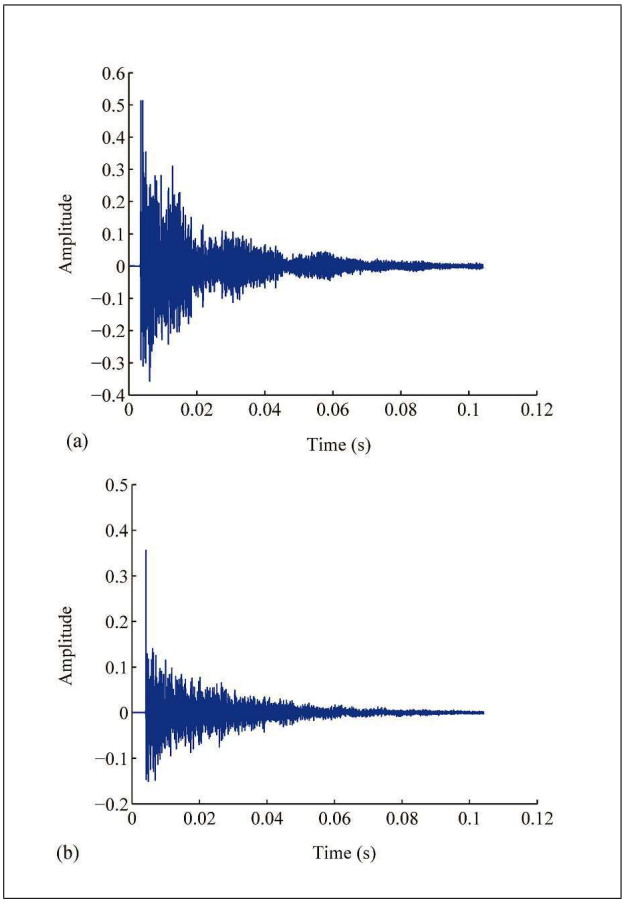

Figure 2. Examples of impact acoustic signals from an undamaged wheat kernel (a) and an IDK (b).

2. Apply EMD to $X_i(t)$, then each of the IMF components $c_{j,i}$ can be obtained, where $c_{j,i}$ represents the jth IMF component of the ith trial.
3. Add a different white noise series $\omega_i(t)$ to the original signals, and repeat steps (1) and (2) until K trials.
4. Calculate the ensemble mean of K trials,

$$c_j(t) = \frac{1}{K}\sum_{i=1}^{K} c_{j,i}(t), \tag{2}$$

$j = 1, 2, \ldots, m$, $i = 1, 2, \ldots, K$, where m is the number of IMF components.

5. Eventually, the original signal $x(t)$ can be represented as

$$x(t) = \sum_{j=1}^{m} c_j(t) + r_m(t), \tag{3}$$

where $c_j(t)$ represents the jth IMF component, and $r_m(t)$ is the residue.

Generally, the result of decomposition will be closer to the actual value if more trials are taken. Usually, $K = 100$.

Typical impact acoustic signals from an undamaged wheat kernel and an IDK are shown in Figure 2. Compared with the signal from the IDK, the signal from the undamaged wheat kernel may have a larger peak value, but the peak values of the signals are quite variable so they are not very useful for distinguishing IDK from undamaged wheat kernels. However, the signals of undamaged wheat kernels typically have larger fluctuation during the resonance decay process. Relative to the signals of undamaged wheat kernels, the signals of IDK have more stable decay trends, associated with the intrinsic characteristics and the resonance effects of their impacts on the steel plate.

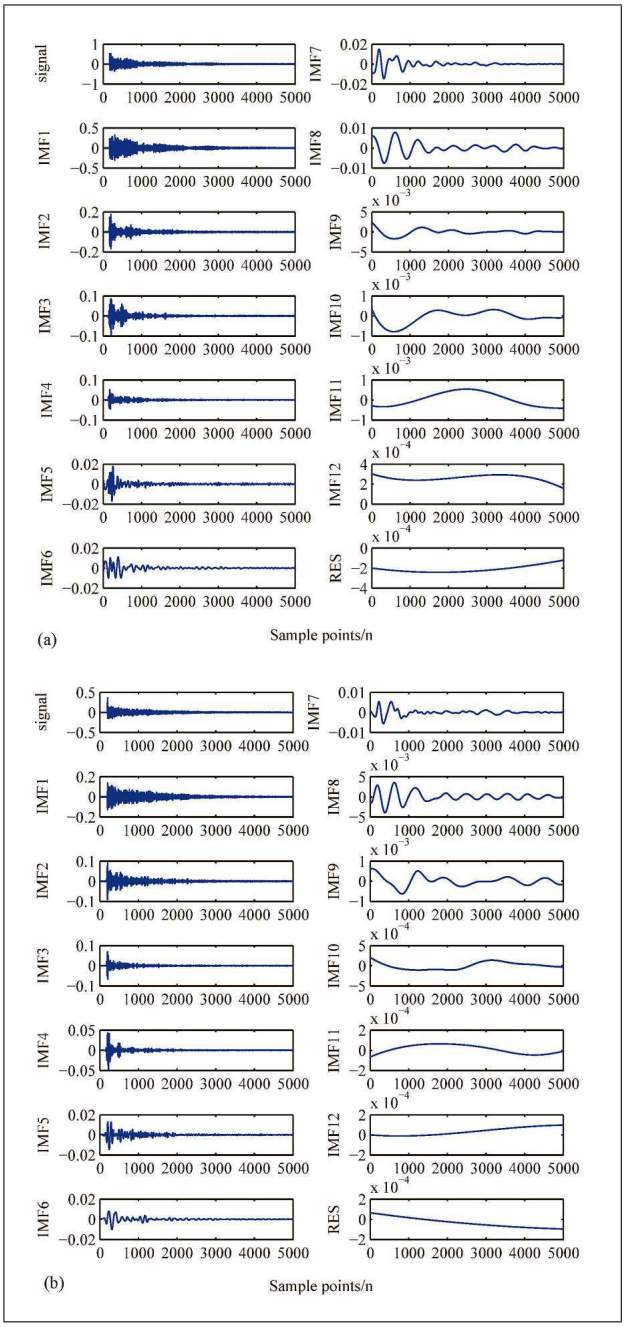

Figure 3. EEMD of the signals from an undamaged wheat kernel (a) and an IDK (b).

Figure 3 demonstrates the EEMD of the signals from an undamaged wheat kernel and an IDK. The main signal energy exists in the first several IMF components. This characteristic indicates that the features should be extracted in the first several IMFs.

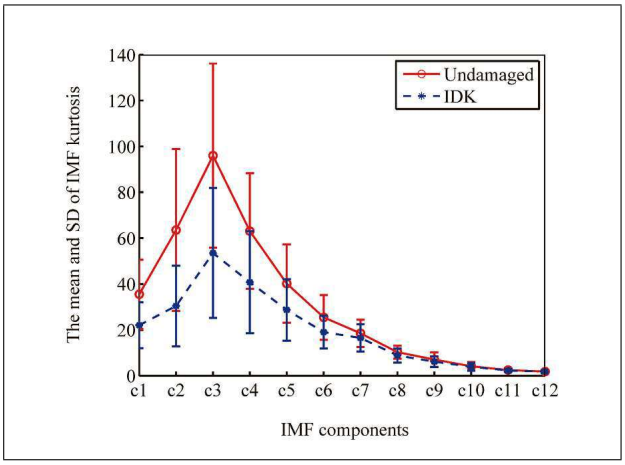

Figure 4. The mean and SD (dot and error bars) of IMF kurtosis for 300 undamaged wheat kernels and 300 IDK.

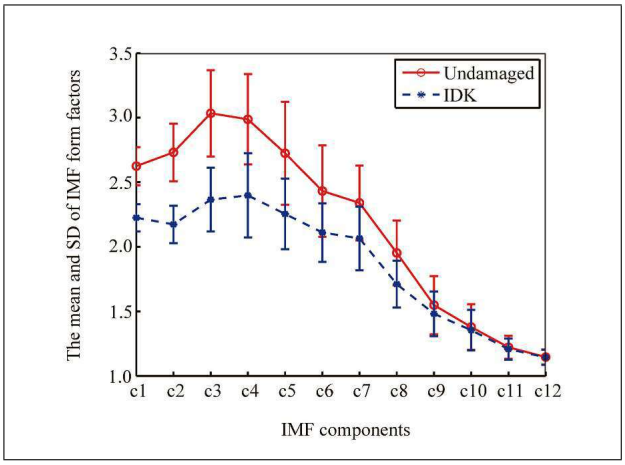

Figure 5. The mean and SD of IMF form factors for 300 undamaged wheat kernels and 300 IDK.

4. Results

4.1. Feature extraction by EEMD method

In this paper, 5000 data points were acquired for each impact, beginning 20 points before the maximum magnitude of the whole signal. The IMF kurtosis, IMF form factors, IMF third-order Rényi entropies, as well as the mean of the degree of stationarity were extracted as the discriminant features. The details of feature extraction are as follows:

4.1.1. The IMF kurtosis

The kurtosis, a dimensionless parameter, reflects the distribution characteristics of signals. For a discrete signal, the IMF kurtosis can be expressed as

$$\mathrm{Kurt}_{c_j} = \frac{1}{N}\sum_{k=1}^{N}\frac{\left(c_{j,k}-\bar{c}_j\right)^4}{\sigma_{c_j}^4}, \tag{4}$$

where $c_{j,k}$ represents the kth data point of the jth IMF, $\bar{c}_j$ is the average of the jth IMF, N is the number of data points, and σ_{c_j} is the standard deviation (SD) of the jth IMF. Figure 4 shows the mean and SD of IMF kurtosis for 300 undamaged wheat kernels and 300 IDK. Before the 7th IMF component, the mean of IMF kurtosis for undamaged wheat kernels are larger than for IDK. However, there is little information in the last several IMF components. The first 6 IMF kurtosis components were extracted for inclusion as discriminant features.

4.1.2. The IMF form factors

Form factors reflect distributional characteristics of signals in the time domain. For a discrete signal, the IMF form factors are represented as

$$K_{f_{c_j}} = \frac{\sqrt{\frac{1}{N}\sum_{k=1}^{N}c_{j,k}^2}}{\frac{1}{N}\sum_{k=1}^{N}\left|c_{j,k}\right|}, \tag{5}$$

where $c_{j,k}$ represents the kth data point of the jth IMF, and N is the number of data points.

Figure 5 shows the mean and SD of IMF form factors for 300 undamaged wheat kernels and 300 IDK. The change trends of the mean of IMF form factors for undamaged kernels and IDK are generally similar. The two types of kernel can be distinguished because the mean of IMF form factors for undamaged wheat kernels are larger than for IDK before the 9th IMF. The first 8 IMF form factors were extracted as discriminant features.

4.1.3. The IMF third-order Rényi entropy

For the jth IMF component c_j ($j = 1, 2, \ldots, m$), the IMF Rényi entropy is

$$R_\alpha(c_j) = \frac{1}{1-\alpha}\ln\left(\sum_{k=1}^{N}P_{c_{j,k}}^{\alpha}\right), \tag{6}$$

where α is the order of Rényi entropy, here $\alpha > 0$ and $\alpha \neq 1$. For $\alpha \to 1$ with restriction of reaching 1, it reduces to the Shannon entropy. N is the number of data points, and $P_{c_{j,k}}$ is the probability density,

$$P_{c_{j,k}} = c_{j,k}^2 \Big/ \sum_{k=1}^{n}c_{j,k}^2, \tag{7}$$

where $c_{j,k}$ is the kth data point of the jth IMF component.

Several empirical studies indicated that in addition to appearing immune to the negative time frequency representation values that can invalidate the Shannon approach, the third-order Rényi entropy seemed to measure signal complexity [22], so the IMF third-order Rényi entropies were computed for this report. Figure 6 shows the mean and SD of IMF third-order Rényi entropies for 300 undamaged wheat kernels and 300 IDK. The curves of the two types present a general upward trend, and it is evident that the mean of IMF third-order Rényi entropies are greater for IDK than for undamaged wheat kernels before the 7th IMF component. Compared with the signals from undamaged wheat kernels, the signals from IDK have a more stable decay trend (Figure 2); therefore, the relative complexities and the IMF third-order Rényi entropies for

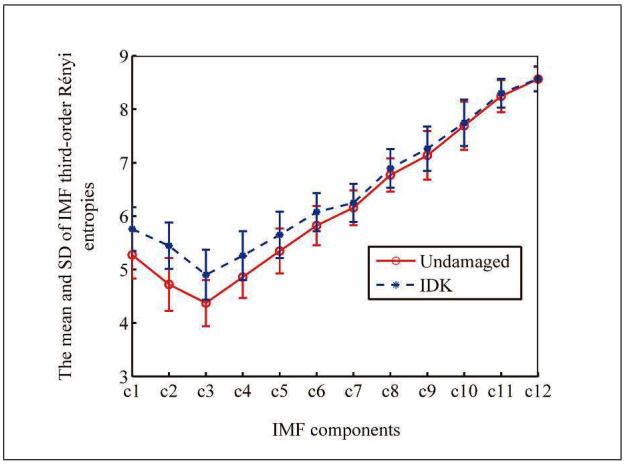

Figure 6. The mean and SD of IMF third-order Rényi entropies for 300 undamaged wheat kernels and 300 IDK.

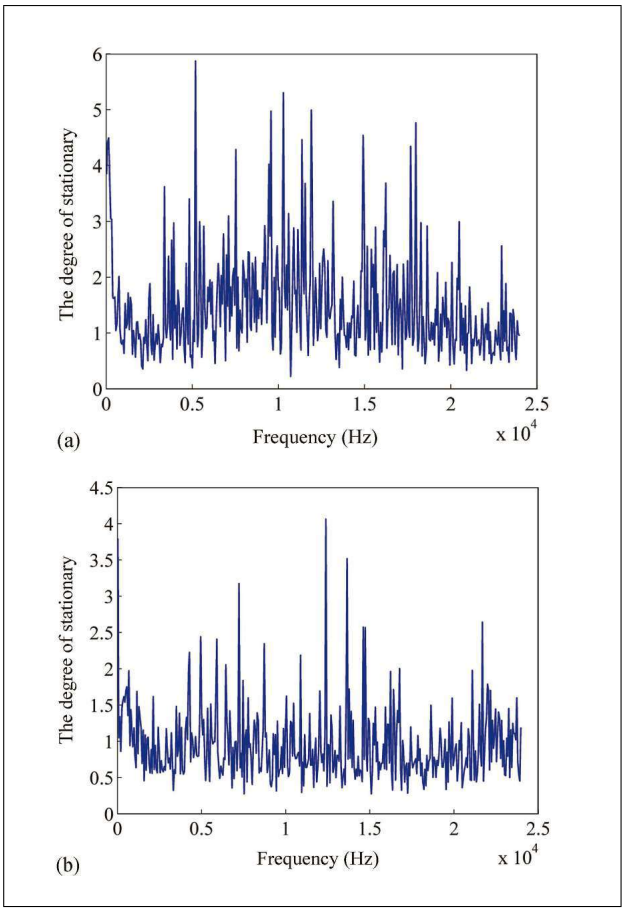

Figure 7. The degree of stationarity from an undamaged wheat kernel (a) and an IDK (b).

IDK are larger. This characteristic provides us with good detection features. The first 6 IMF third-order Rényi entropies were extracted as discriminant features.

4.1.4. The mean of the degree of stationarity

The Hilbert transform of the jth IMF $c_j(t)$ is

$$y_j(t) = \frac{1}{\pi} P \int_{-\infty}^{\infty} \frac{c_j(\tau)}{t-\tau}\,\mathrm{d}\tau, \tag{8}$$

where P is the Cauchy principal value, and the analytic signal $z_j(t)$ is defined as

$$z_j(t) = c_j(t) + \mathrm{i}y_j(t) = a_j(t)\exp\left(\mathrm{i}\theta_j(t)\right), \tag{9}$$

where

$$a_j(t) = \sqrt{\left(c_j(t)\right)^2 + \left(y_j(t)\right)^2},$$
$$\theta_j(t) = \arctan\left(y_j(t)/c_j(t)\right),$$

and the instantaneous frequency is defined as

$$\omega_j(t) = \frac{\mathrm{d}\theta_j(t)}{\mathrm{d}t}. \tag{10}$$

Applying the Hilbert transform to each IMF, the original signal $x(t)$ can be expressed as

$$x(t) = \sum_{j=1}^{m} a_j(t)\exp\left(\mathrm{i}\theta_j(t)\right) = \sum_{j=1}^{m} a_j(t)\exp\left(\mathrm{i}\int \omega_j(t)\,\mathrm{d}t\right). \tag{11}$$

Here the residue, $r_m(t)$, is left out, because it is either a monotonic function or a constant. Equation (11) also enables us to represent the amplitude and the instantaneous frequency as functions of time. The frequency-time distribution of the amplitude is called Hilbert amplitude spectrum, $H(\omega, t)$, or simply Hilbert spectrum. Define the marginal spectrum, $h(\omega)$, as

$$h(\omega) = \int_0^N H(\omega, t)\,\mathrm{d}t, \tag{12}$$

then the mean marginal spectrum, $n(\omega)$, is

$$n(\omega) = h(\omega)/N, \tag{13}$$

where, for a discrete signal, N represents the number of data points.

The degree of stationarity is defined as

$$\mathrm{DS}(\omega) = \frac{1}{N}\int_0^N \left(1 - \frac{H(\omega, t)}{n(\omega)}\right)^2 \mathrm{d}t. \tag{14}$$

For DS(ω), the higher the index value, the more non-stationary is the process [17]. Distributions of the degree of stationarity from an undamaged wheat kernel and an IDK are shown in Figure 7. The degree of stationarity is quite variable in different frequency ranges whether for the undamaged wheat kernel or the IDK. The degree of stationarity for the undamaged wheat kernel tends to remain larger than for the IDK, so we adopted the mean of the degree of stationarity as one of the discriminant features.

The mean values and SDs of the partial discriminant features of signals for randomly selected 300 undamaged wheat kernels and 300 IDK are shown in Table I for the first 4 IMF components, $c_1 \ldots c_4$, of the kurtosis, form factor, and Rényi entropy, as well as the mean of the degree of stationarity. The mean values and SDs from all features

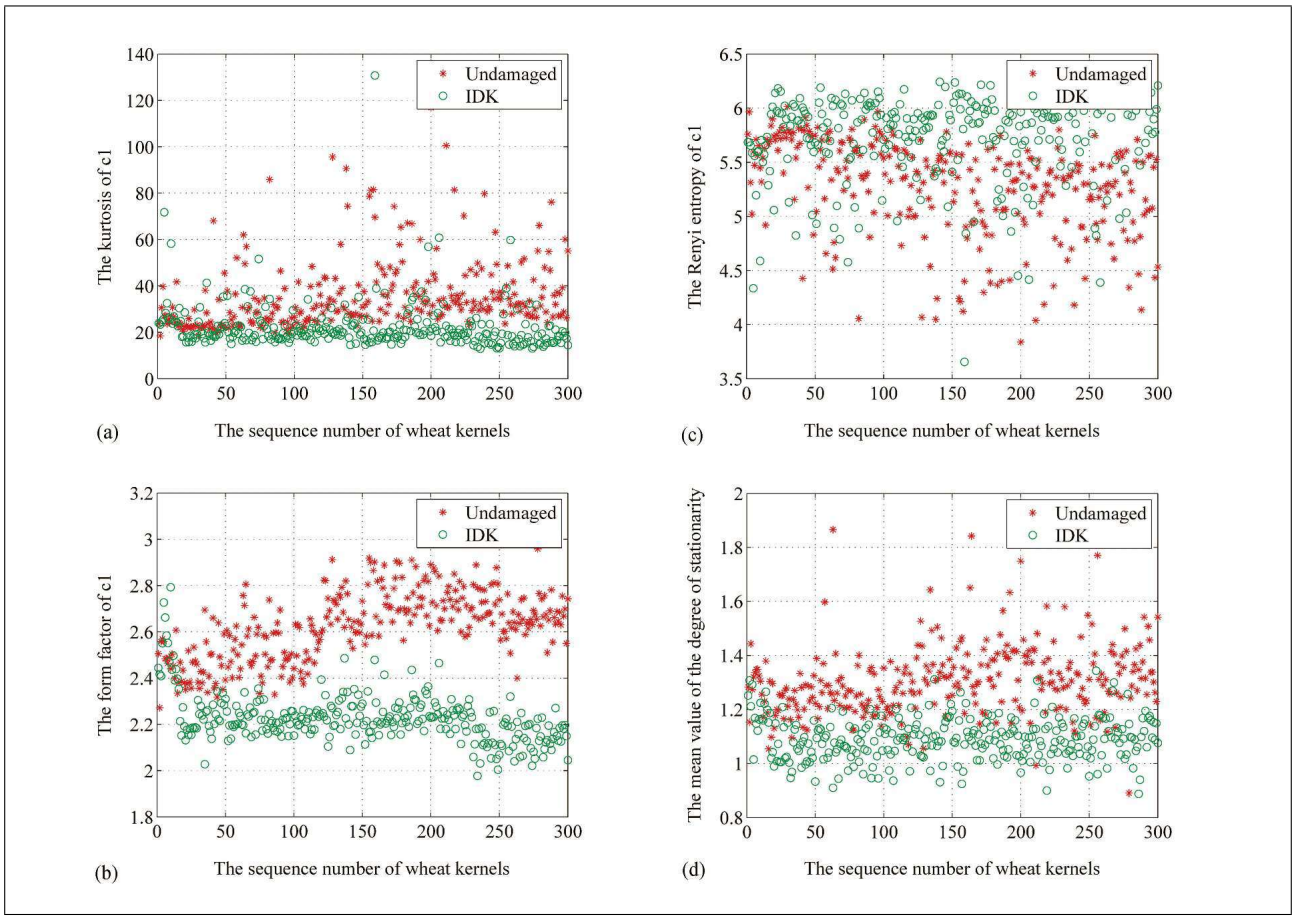

Figure 8. Scatter diagram of partial discriminant features from undamaged wheat kernels and IDK.

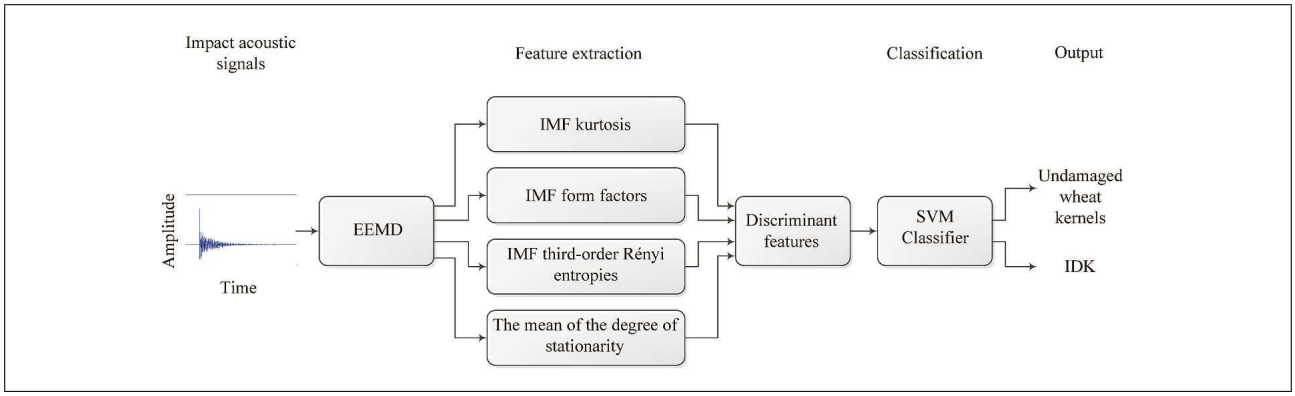

Figure 9. Block diagram of the detection process.

indicate that the extracted features enable good separation of differences between the two types of wheat kernels. Visual representations are presented in Figure 8, where the red marks and the green marks represent the feature values of undamaged wheat kernels and IDK, respectively. These characteristics indicate that IDK can be distinguished successfully from undamaged wheat kernels by using the selected features.

Figure 9 shows the block diagram of the detection system. The Matlab data acquisition toolbox was used for saving the impact acoustic signals of undamaged wheat kernels and IDK. Based on its capability to process non-stationary signals and its suppression of mode mixing, the EEMD scheme was adopted. Theoretically, when the amplitude of noise remains below a certain level, the results of decomposition will be closer to the actual value if more trials are taken, in this case, 100. The data acquired from EEMD were saved as .mat files, making it more convenient for feature extraction.

The main objects in the study are undamaged wheat kernels and IDK. For each type, 300 wheat kernels were used with 150 for training and 150 for testing. The wheat kernels were not screened through any means.

Table I. Partial feature statistics from 300 undamaged wheat kernels and 300 IDK Features.

	Undamaged wheat kernels		IDK	
	Mean	SD	Mean	SD
IMF kurtosis (c_1)	35.47	15.16	22.00	10.01
IMF kurtosis (c_2)	63.54	35.36	30.40	17.58
IMF kurtosis (c_3)	95.96	40.14	53.52	28.31
IMF kurtosis (c_4)	63.08	25.19	40.76	22.28
IMF form factor (c_1)	2.63	0.15	2.23	0.11
IMF form factor (c_2)	2.73	0.22	2.17	0.15
IMF form factor (c_3)	3.03	0.33	2.37	0.25
IMF form factor (c_4)	2.99	0.35	2.40	0.33
IMF third-order Rényi entropy (c_1)	5.27	0.44	5.76	0.41
IMF third-order Rényi entropy (c_2)	4.72	0.50	5.44	0.43
IMF third-order Rényi entropy (c_3)	4.37	0.43	4.90	0.47
IMF third-order Rényi entropy (c_4)	4.86	0.39	5.26	0.46
The mean of the degree of stationarity	1.31	0.13	1.09	0.08

Table II. Classification accuracies for subsets of features.

Features	Number of features	Classification accuracy (%)	
		Undamaged	IDK
I. Rényi entropy	6	92.0	74.0
II. Kurtosis	6	94.7	82.7
III. Stationarity average	1	91.3	88.7
IV. Form factor	8	99.3	91.3
I+II	6+6	96.0	85.3
I+III	6+1	5.3	87.3
I+IV	6+8	98.7	92.7
II+III	6+1	96.7	86.0
II+IV	6+8	97.3	93.3
III+IV	1+8	98.7	91.3
I+II+III	6+6+1	98.0	87.3
I+II+IV	6+6+8	97.3	93.3
I+III+IV	6+1+8	98.0	92.7
II+III+IV	6+1+8	98.0	91.3
I+II+III+IV	6+6+1+8	98.7	93.3

4.2. Classification

Based on its superiority of non-linear classification, the SVM software of Libsvm [23] was used in the experiment, and the radial basis function (RBF) was adopted as the SVM kernel function,

$$K\left(\vec{x}_i \cdot \vec{x}_j\right) = \exp\left(-\gamma \left\| \vec{x}_i - \vec{x}_j \right\|^2\right). \quad (15)$$

The radial basis function can be a better choice relative to the linear kernel function, because it can deal with the circumstance where the relation between class labels is nonlinear. For the SVM classifier, the penalty factor, C, and the kernel function, γ, are important parameters. The grid-search (GS) algorithm [24] was adopted for selecting the optimal penalty factor and kernel function parameters by finding the values giving the highest ten-fold cross-validation accuracy in the training set (containing 150 undamaged wheat kernels and 150 IDK). For this experiment, the best C and γ were determined to be 256 and 0.0625, respectively. Different colors reflect percentage accuracy differences (Figure 10).

Table III. SVM Classification accuracies when using different methods for parameter selection.

Method for SVM parameter selection	Classification accuracy (%) Undamaged	IDK
Default parameters	98.0	91.3
Grid-search with ten-fold cross-validation	98.7	93.3

Different combinations of the classification features are shown in Table II for identification of subsets of optimal features. When only one type of feature is considered, the IMF form factors can be regarded as the optimal features, achieving 99.3% detection accuracy for undamaged wheat kernels and 91.3% for IDK. Using these features alone, clear differences between undamaged kernels and IDK are evident, and the features are beneficial particularly for detection of undamaged wheat kernels. However, when all 21 discriminant features are used, the undamaged kernels

Table IV. Classification outcomes for SVM to detect undamaged wheat kernels and IDK, with additional types of damaged wheat kernels (300 scab-damaged and 300 sprout-damaged) included in experiment.

Damage category	Classification outcome (%)			
	Undamaged	Insect-damaged	Scab-damaged	Sprout-damaged
Undamaged	87.3	1.3	10.7	0.7
Insect-damaged	6.7	77.3	6.7	9.3
Scab-damaged	14.0	14.7	66.7	4.6
Sprout-damaged	5.3	5.3	9.4	80.0

Table V. Comparison study of the conventional and selected methods.

Method	Number of features	Classification accuracy (%)		Processing time (s/kernel)
		Undamaged	IDK	
Conventional method	29	94.7	89.3	0.05
Selected method	21	98.7	93.3	0.34

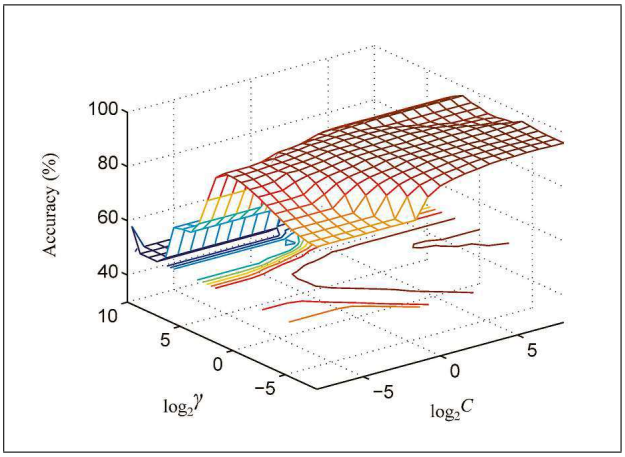

Figure 10. Grid-search algorithm with ten-fold cross-validation for optimal parameters selection (the best $C = 256$, the best $\gamma = 0.0625$).

and IDK both are classified with high accuracy, achieving 98.7% for undamaged wheat kernels and 93.3% for IDK, which improved the effectiveness of the proposed method. Table III reports the detection accuracy with different methods for parameter selection when using all 21 features included in the SVM.

Table IV reports the classification outcomes for an additional data set including the original 300 undamaged wheat kernels and 300 IDK combined with 300 additional scab-damaged and 300 sprout-damaged wheat kernels. The results indicated that the proposed method can classify four types of wheat kernel with > 60% accuracy.

For further study, a comparative study was conducted with the addition of two analyses: 1) computing the short-time window variances and maxima of the impact acoustic signals, 2) analysis of the frequency spectra magnitudes. For the short-time window variances and maxima computations, we used 8 short-time windows which were 150 points in duration and incremented in steps of 120 points so that each window was overlapped by 30 points. The first window began 20 points before the maximum magnitude. Then, all the short-time window variances and maxima were normalized. For frequency spectra magnitudes computations, the maximum magnitude and the 6 spectrum-level values before and after the maximum were computed and normalized.

Finally, a total of 29 normalized features, including 8 short-time variances, 8 short-time maximums, and 13 frequency spectra magnitudes, were used as inputs to the SVM, and the RBF kernel parameters as well as the penalty factor were optimized with the grid-search algorithm by finding the values giving the highest ten-fold cross-validation accuracy in the training set. Table V shows the results of the comparison study. Here, "Conventional method" means extracting 29 features as described above, "Selected method" means extracting 21 features through EEMD method as in Table 2. The results indicated that the selected method developed in this report can obtain better detection accuracies for undamaged wheat kernels and IDK than the conventional method.

5. Discussion

In this report, important features of impact acoustic signals were extracted by using an EEMD method. Although the kurtosis, form factors and third-order Rényi entropy features can also be extracted from original impact acoustic signals in the time domain, this extraction is done by a procedure that reflects the general characteristics of signals rather than the local characteristics. However, feature extraction through EEMD method can reveal the different IMFs over which the features are separable for different wheat kernel types and thus are useful for classification. The discriminant features are separable in the first several IMFs, but not in the last several IMFs. Based on this characteristic, the discriminant features should be extracted from the first several IMFs.

It should be noted that the throughput of the system in this paper is not rapid, approximately 0.34 s for processing of each wheat kernel (Table 5). However, it is an

acceptable throughput in this case because it matches the processing speed of the experimental apparatus. Also, the detection system has high accuracy, achieving 98.7% for undamaged wheat kernels and 93.3% for IDK. In addition, the detection system is easy to acquire and low-cost. Therefore, the system is suitable for small-sample detection for which the throughput is not demanded very high but high precision is indeed required. For example, the US Grain Inspection Service, Packers, and Stockyard Administration (GISPSA) guidelines classify samples through sieving and visually inspecting a sample (1 kg) to detect the insects inside wheat kernels and determine the quality of a particular shipment [25]. The method proposed in this paper for detection of IDK is suitable for this work.

6. Conclusion and future work

In this paper, a new method based on EEMD analysis of impact acoustics was developed for detection of IDK. The features, including the IMF kurtosis, IMF form factors, IMF third-order Rényi entropies, and the mean value of the degree of stationarity enabled good detection accuracies.

The new method has the following characteristics:

1. EEMD, which is based on the local characteristic time scales of a signal, can self-adaptively processes nonstationary signals and suppresses mode mixing.
2. SVM can be used for classification, with 98.7% of undamaged wheat kernels and 93.3% of insect-damaged ones detected correctly.
3. When other types of damaged wheat kernels are added to the data set for classification, the proposed method can still detect undamaged wheat kernels and IDK with $> 60\%$ accuracy.

In future work, further technical details can be studied. For instance, we can evaluate the detection performance in various controlled circumstances, such as the temperature, the size of wheat kernels, and the level of maturity. Also, we can improve the recognition rates for multi-class classification.

Acknowledgement

This work was supported by the National Natural Science Foundation of China (No. 11172342, 11372167), the Science Research and Development Program of Shaanxi Province of China (No. 2016NY-176), the Fundamental Research Funds for the Central Universities (No. GK 201405007) and Interdisciplinary Incubation Project of Learning Science of Shaanxi Normal University.

References

[1] M. Guo, Z. Shang, H. Shi: Sound absorption measurements of various types of grain. Acta Acustica united with Acustica **91** (2005) 915–919.

[2] T. C. Pearson, A. E. Cetin, A. H. Tewfik: Detection of insect damaged wheat kernels by impact acoustics. Proceedings of IEEE International Conference on Acoustics, Speech, and Signal Processing (ICASSP'05), Philadelphia, Pennsylvania, USA, 2005, 649–652.

[3] T. C. Pearson: Detection of pistachio nuts with closed shells using impact acoustics. Applied Engineering in Agriculture **17** (2001) 249–253.

[4] A. E. Cetin, T. C. Pearson, A. H. Tewfik: Classification of closed- and open-shell pistachio nuts using voice-recognition technology. Transactions of the ASABE **47** (2004) 659–664.

[5] R. P. Haff, T. C. Pearson: Separating in-shell pistachio nuts from kernels using impact vibration analysis. Sensing and Instrumentation for Food Quality and Safety **1** (2007) 188–192.

[6] M. Omid, A. Mahmoudi, M. H. Omid: An intelligent system for sorting pistachio nut varieties. Expert Systems with Applications **36** (2009) 11528–11535.

[7] M. Omid, A. Mahmoudi, M. H. Omid: Development of pistachio sorting system using principal component analysis (PCA) assisted artificial neural network (ANN) of impact acoustics. Expert Systems with Applications **37** (2010) 7205–7212.

[8] M. Omid: Design of an expert system for sorting pistachio nuts through decision tree and fuzzy logic classifier. Expert Systems with Applications **38** (2011) 4339–4347.

[9] I. Onaran, T. C. Pearson, Y. Yardimci, A. E. Cetin: Detection of underdeveloped hazelnuts from fully developed nuts by impact acoustics. Transactions of the ASABE **49** (2006) 1971–1976.

[10] H. Kalkan, N. F. Ince, A. H. Tewfik, Y. Yardimci, T. C. Pearson: Classification of hazelnut kernels by using impact acoustic time-frequency patterns. EURASIP Journal on Advances in Signal Processing **2008** (2008) 1–11.

[11] A. E. Cetin, T. C. Pearson, R. A. Sevimli: System for removing shell pieces from hazelnut kernels using impact vibration analysis. Computers and Electronics in Agriculture **101** (2014) 11–16.

[12] A. Hosainpour, M. H. Komarizade, A. Mahmoudi, M. G. Shayesteh: Feasibility of impact-acoustic emissions for discriminating between potato tubers and clods. Journal of Food, Agriculture & Environment **8** (2010) 565–569.

[13] A. Hosainpour, M. H. Komarizade, A. Mahmoudi, M. G. Shayesteh: High speed detection of potato and clod using an acoustic based intelligent system. Expert Systems with Applications **38** (2011) 12101–12106.

[14] S. Khalifa, M. H. Komarizadeh: An intelligent approach based on adaptive neuro-fuzzy inference systems (ANFIS) for walnut sorting. Australian Journal of Crop Science **6** (2012) 183–187.

[15] T. C. Pearson, A. E. Cetin, A. H. Tewfik, R. P. Haff: Feasibility of impact-acoustic emissions for detection of damaged wheat kernels. Digital Signal Processing **17** (2007) 617–633.

[16] N. F. Ince, I. Onaran, T. C. Pearson, A. H. Tewfik, A. E. Cetin, H. Kalkan, Y. Yardimci: Identification of damaged wheat kernels and cracked-shell hazelnuts with impact acoustics time-frequency patterns. Transactions of the ASABE **51** (2008) 1461–1469.

[17] N. E. Huang, Z. Shen, S. R. Long, et al.: The empirical mode decomposition and the Hilbert spectrum for nonlinear and non-stationary time series analysis. Proceedings of the Royal Society of London Series A – Mathematical, Physical and Engineering Sciences **454** (1998) 903–995.

[18] Z. Wu, N. E. Huang: Ensemble empirical mode decomposition: a noise-assisted data analysis method. Advances in Adaptive Data Analysis **1** (2009) 1–41.

[19] H. Jiang, C. Li, H. Li: An improved EEMD with multi-wavelet packet for rotating machinery multi-fault diagno-

sis. Mechanical Systems and Signal Processing **36** (2013) 225–239.

[20] Y. Lei, Z. He, Y. Zi: EEMD method and wnn for fault diagnosis of locomotive roller bearings. Expert Systems with Applications **38** (2011) 7334–7341.

[21] H. Hao: Multi component LFM signal detection and parameter estimation based on EEMD-FRFT. Optik **124** (2013) 6093–6096.

[22] R. G. Baraniuk, P. Flandrin, A. J. E. M. Janssen, O. J. J. Michel: Measuring time-frequency information content using the Rényi entropies. IEEE Transactions on Information Theory **47** (2001) 1 391–1 409.

[23] C. C. Chang, C. J. Lin: LIBSVM: A library for support vector machines. ACM Transactions on Intelligent Systems and Technology **2** (2011) 27.

[24] F. J. Pontes, G. F. Amorim, P. P. Balestrassi, et al.: Design of experiments and focused grid search for neural network parameter optimization. Neurocomputing **186** (2016) 22–34.

[25] D. K. Weaver, D. Shuman, R. W. Mankin: Optimizing and assessing the performance of an algorithm that cross-correlates acquired acoustic emissions from internally feeding larvae to count infested wheat kernels in grain samples. Applied Acoustics **50** (1997) 297–308.